Reactivity of Tuck-over Titanium Oxo Complexes with Isocyanides

María Gómez-Pantoja,[†,§] Juan. I. González-Pérez,[†,§] Avelino Martín,[†,§] Miguel Mena,[†,§] Cristina Santamaría*[†,§] and Manuel Temprado[‡,§]

[†] Departamento de Química Orgánica y Química Inorgánica, Universidad de Alcalá, Campus Universitario, 28805 Alcalá de Henares, Madrid, Spain

[‡] Departamento de Química Analítica, Química Física e Ingeniería Química, Universidad de Alcalá, Campus Universitario, 28805 Alcalá de Henares, Madrid, Spain

[§] Instituto de Investigación Química "Andrés M. del Río" (IQAR), Universidad de Alcalá, Campus Universitario, 28805 Alcalá de Henares, Madrid, Spain

Supporting Information

ABSTRACT: The reactivity of the "tuck-over" species [$Ti_2(\eta^5\text{-}C_5Me_5)(CH_2Ph)_3(\mu\text{-}\eta^5\text{-}C_5Me_4CH_2\text{-}\kappa C)(\mu\text{-}O)$] (**1**) and [$Ti_2(\eta^5\text{-}C_5Me_5)(CH_2CMe_3)(\mu\text{-}\eta^5\text{-}C_5Me_4CH_2\text{-}\kappa C)(\mu\text{-}CH_2CMe_2CH_2)(\mu\text{-}O)$] (**2**) towards isocyanides has been examined both synthetically and theoretically. Treatment of **1** with the isocyanides RNC, R = Me_3SiCH_2, 2,6-$Me_2C_6H_3$, *t*Bu, *i*Pr, leds to a series of η^2-iminoacyl species (**3-6**) where the molecule of isocyanide inserts into one of the terminal metal-alkyl bonds. The analogous reaction of the "tuck-over" metallacycle species **2** with 2,6-$Me_2C_6H_3NC$ and *t*BuNC results in the initial insertion of one isocyanide into the terminal Ti-alkyl bond to form the iminoacyl complexes **7** and **8**, followed by a second insertion into the metallacycle moiety to generate **9**, in the case of *tert*-butylisocyanide. DFT calculations support the selective reactivity observed experimentally with a kinetic and thermodynamic preference for RNC insertion on the terminal alkyl groups bound to both metallic centers over the alternative insertion on the "tuck-over" ligand.

INTRODUCTION

C-H activation of a $\eta^5\text{-}C_5Me_5$ ligand is not as surprising as was initially thought. Since the pioneering works of Britzinger and Bercaw in the 1970's about the tetramethylfulvene derivatives [$Ti(\eta^5\text{-}C_5Me_5)\{C_5Me_4(CH_2)\}R$] (R = Me,[1,2] H[3]) and later the proposal suggested by Watson of the tuck-in intermediate "[$Lu(\eta^5\text{-}C_5Me_5)\{C_5Me_4(CH_2)\}$]" in the homogeneous activation of methane,[4,5] there is now considerable precedent in the literature for this type of metalated pentamethylcyclopentadienyl complexes.[6-13] Moreover, the description of the permethylated ligand as $\eta^4{:}\eta^2$ bonding in a fulvene formulation or as $\eta^5{:}\eta^1$ bonding in a tucked-in ligand have extensively been illustrated.[6]

An alternative type of activation of the pentamethylcyclopentadienyl ligand in which the methylene group formed by C-H activation is attached to a second metal atom has been less studied. The first crystallographically characterized tuck-over derivative in the literature, [$Ti_2(\eta^5\text{-}C_5Me_5)_2(\mu\text{-}\eta^5\text{-}C_5Me_4CH_2\text{-}\kappa C)(\mu\text{-}O)_2$], was obtained by the reaction of N_2O and a toluene solution of [$Ti(\eta^5\text{-}C_5Me_5)_2$].[14] In contrast to the tuck-in analogous, which exhibited interesting reactivity,[15-23] Bottomley's showed a remarkable inertness toward O_2, CO, ethylene or even H_2.[24] Later, Evans reported the crystal structure of [$(\eta^5\text{-}C_5Me_5)_2Lu(\mu\text{-}H)(\mu\text{-}\eta^5\text{-}C_5Me_4CH_2\text{-}\kappa C)Lu(\eta^5\text{-}C_5Me_5)$],[25] a tuck-over complex of a f-block element. Examples of many f-block tuck-in and tuck-over complexes have now been reported with extensive reactivity.[26,27]

Our research group has found that the thermal treatment of the tetralkyl dinuclear complexes [$Ti(\eta^5\text{-}C_5Me_5)R_2]_2(\mu\text{-}O)$ (R = CH_2Ph, CH_2CMe_3) led to an intramolecular C-H activation resulting in the formation of alkane (RH) and the crystallographically characterized tuck-over complexes, [$Ti_2(\eta^5\text{-}C_5Me_5)(CH_2Ph)_3(\mu\text{-}\eta^5\text{-}C_5Me_4CH_2\text{-}\kappa C)(\mu\text{-}O)$] (**1**) and [$Ti_2(\eta^5\text{-}C_5Me_5)(CH_2CMe_3)(\mu\text{-}\eta^5\text{-}C_5Me_4CH_2\text{-}\kappa C)(\mu\text{-}CH_2CMe_2CH_2)(\mu\text{-}O)$] (**2**).[28] Herein, we now report the results of the reactivity of these species towards isocyanides and considerations of the insertion processes on the basis of DFT calculations.

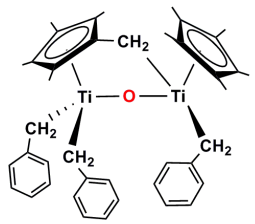

(1)

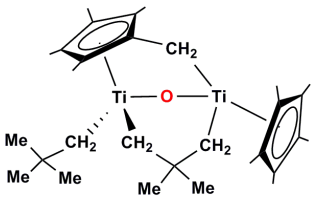

(2)

RESULTS AND DISCUSSION

Addition of RNC, R = 2,6-$Me_2C_6H_3$, Me_3SiCH_2, *t*Bu, *i*Pr, at room temperature to a hexane or toluene solution of **1** in 1:1 molar ratio or an excess, and cooling at -20 °C for several days, enabled selective monoinsertion, and complexes **3-6** were isolated as red (**3-5**) or reddish-orange (**6**) solids in low-moderate yields (35-57 %), as outlined in Scheme 1. Compounds **3-6** show thermal instability in solution (degradation is observed after few minutes at room temperature) leading to an intractable mixture of products and, therefore, they must be stored in solid state at low temperatures (< -20 °C). The monoinsertion processes were characterized by ^{1}H (**4-6**) and 2D gHSQC (**5**, **6**) experiments, IR spectroscopy and elemental analysis. The confirmation of their molecular structures, relative position and bonding of the molecule of isocyanide, came from the X-ray diffraction analysis for **3-5**.

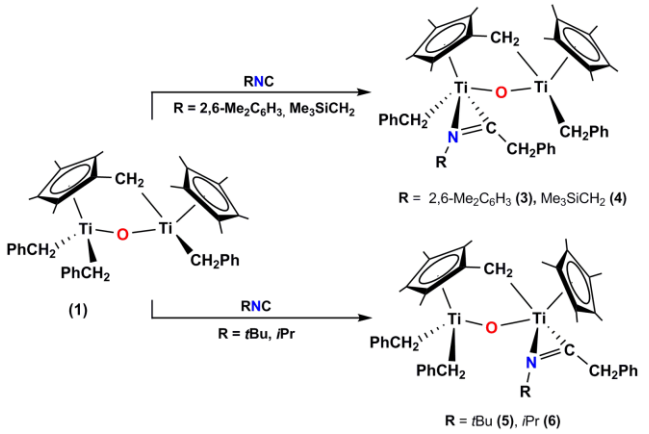

Scheme 1. Reactivity of complex **1** with isocyanides.

Crystals of **3-5** suitable for X-ray diffraction were grown from a concentrated toluene (**3**) or hexane (**4**, **5**) solutions stored at -20 °C for several days. The crystal structures are shown in Figure 1, and selected bond lengths and angles of each complex are listed in Table 1. As shown in Figure 1, the solid-state structures of these compounds show a (μ-η^5-$C_5Me_4CH_2$-κC) ligand engaged in a tuck-over binding mode to the titanium atoms and clear up that the insertion of the isocyanide molecule only has taken place into a titanium-benzyl bond. Curiously, complex **5** shows the insertion of the isocyanide molecule into the unique Ti2-CH_2Ph bond, while complexes **3** and **4** experienced it at the adjacent metal center. Additionally, the η^2-iminoacyl moiety in **4** exhibits an *exo* disposition while in **3** adopts an *endo* configuration, favored by the existence of two π stacking interactions in this compound (for more details see Figure S1 and Table S2 in Supporting Information).

Each metal center exhibits different structural environments; the five-coordinated titanium atom is in typical four-legged piano-stool geometry while the other adopts a three-legged piano-stool one. Geometrical parameters for the Ti-η^2-iminoacil bonding system are in the range found for monocyclopentadienyl titanium complexes.[29-35] The coordination to titanium of this group increases the electronic density on the metal center and elongates one of the Ti-O distances, although being both comparable with those of the dinuclear starting complexes **1** and **2** and other organometallic dinuclear or trinuclear titanium oxoderivatives (Ti-O = 1.83(2) Å)[36-42]. Additionally, the presence of the η^2-iminoacyl fragment makes longer the distances Ti···Ti and the Ti-O-Ti angles are opened between 2-6° with respect to **1**. Moreover, while the Ti-$CH_2C_5Me_4$ bond lengths of compounds **3** (2.142(4) Å) and **4** (2.134(6)Å) compare well with other titanium(IV)-C(sp^3) σ bond species, the existence of the iminoacyl ligand in **5** elongates this distance to 2.243(6) Å due to a major electronic density and steric hindrance around Ti2.

Table 1. Selected Lengths (Å) and Angles (°) for **1**, **3**, **4**, and **5**.

Complexes	**1**	**3**	**4**	**5**
Ti1-O1	1.809(2)	1.852(3)	1.886(4)	1.797(4)
Ti2-O1	1.828(2)	1.800(3)	1.769(4)	1.853(4)
Ti···Ti	3.208(1)	3.271(1)	3.244(5)	3.307(1)
Ti-N1	---	2.085(3)	2.041(5)	2.122(5)
Ti-$CH_2C_5Me_4$	2.158(3)	2.142(4)	2.134(6)	2.243(5)
N1-C61/C1	---	1.266(5)	1.246(6)	1.276(7)
Ti-C61/C1	---	2.085(4)	2.070(6)	2.073(6)
Ti-CH_2Ph	2.159(3) 2.148(3) 2.128(3)	2.196(4) 2.133(4)	2.177(6) 2.146(6)	2.142(5) 2.141(6)
Ti1-O1-Ti2	123.8(1)	127.2(2)	125.1(2)	129.9(2)
Ti2-C16-C11	105.3(2)	106.4(3)	106.5(4)	110.4(3)

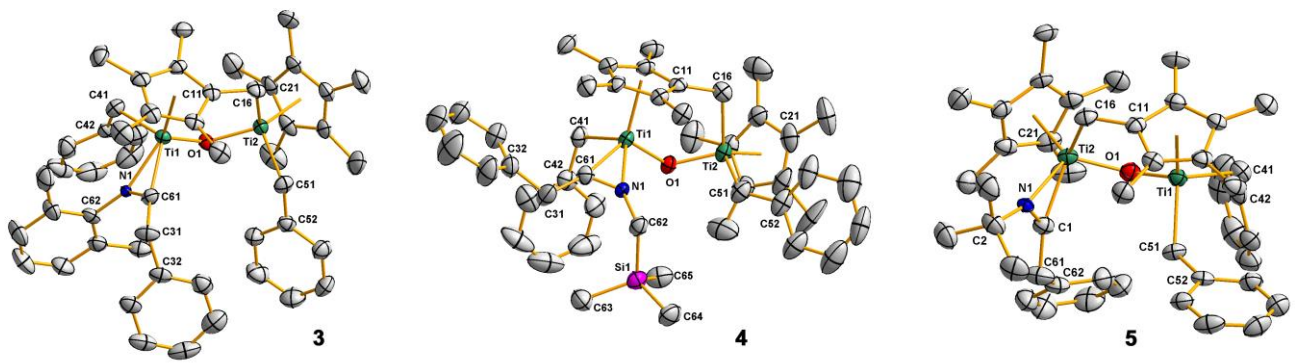

Figure 1. From left to right, ORTEP plots for complexes **3**, **4**, and **5**. Thermal ellipsoids set at 50% probability. All hydrogen atoms are omitted for clarity.

The ^{1}H NMR spectrum of complexes **3-6** in solution displays the same splitting pattern for the five-membered rings, consisting of one η^5-C_5Me_5 signal (δ = 1.69-1.87), four nonequivalent methyl groups (δ = 1.05-2.10), and a diastereotopic methylene for the (μ-η^5-$C_5Me_4CH_2$-κC)$^{2-}$ ligand, in a similar region to that found for the starting compound **1**. Also, the spectra reveal $PhCH_2$ groups linked to titanium and the characteristic signals assigned to the alkyl/aryl substituents N*R*=C-CH_2*Ph* (R = 2,6-$Me_2C_6H_3$, Me_3SiCH_2, *t*Bu and *i*Pr). The existence of the η^2-iminoacyl ligand is confirmed by a stretching band for the C=N bond in the range 1585-1593 cm^{-1} in the IR spectra.[29-35]

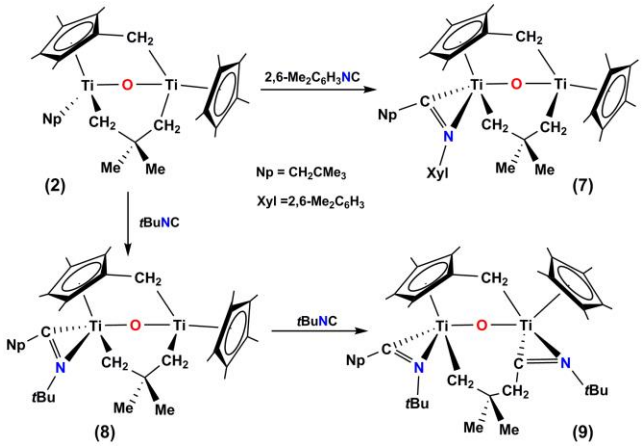

Scheme 2. Reactivity of complex **2** with isocyanides.

Complex **2** also reacts quickly with 1 equiv of 2,6-dimethylphenyl or *tert*-butyl isocyanide to generate compounds **7** and **8** (Scheme 2) as reddish orange solids in high yields (over 80%). These compounds are soluble in common solvents such as hexane, toluene, or thf and turned out to be stable in the crystalline state at room temperature under an argon atmosphere. The products were widely characterized by the usual spectroscopic technics and elemental analysis, but the definitive identification was not possible till the single crystal X-ray diffraction study of compound 7 was carried out after crystallization from hexane. The molecular structure is shown in Figure 2 and selected data in Table 2.

This species shows some structural analogies to the starting compound **2**, and confirms the preference of the isocyanide molecule to be inserted into the Ti-neopentyl bond. Once again, both metal centers exhibit different geometries, while Ti1 shows a typical four-legged piano-stool geometry, Ti2 adopts a three-legged piano-stool geometry, in a similar way to those observed for complexes **3-5**. On the other hand, the planes of the C11-C15 and C21-C25 rings show an angle of 76.3(4)° in order to minimize the steric hindrance. Additionally, the 2,2-dimethylpropane-1,3-diyl fragment adopts an angle of 18.6(1)° with the C11-C15 ring.

The existence of the η^2-iminoacyl ligand opens ≈2° the bond angle Ti1-O1-Ti2 (116.2(1)°) with respect to compound **2** (114.1(1)°) and, therefore, a larger Ti1-O1 bond distance (1.841(2) Å) and a shorter Ti2-O1 length (1.802(3) Å) are observed, according with a different number of electrons at the metal centers. The higher electron density at Ti1 also makes Ti1-C31 (2.212(4) Å) ≈0.1 Å longer than Ti2-C33 (2.108(4) Å), being the latter similar to that found in **2**. Again, the geometrical parameters for the Ti-η^2-iminoacil bonding system are in the range found for monocyclopentadienyl titanium complexes.[29-35]

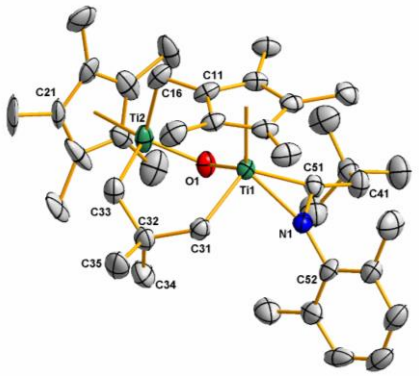

Figure 2. ORTEP plot of **7**. Thermal ellipsoids set at 50% probability. All hydrogen atoms are omitted for clarity.

Table 2. Selected Lengths (Å) and Angles (°) for **2**, **7**, and **9**.

Complexes	**2**	**7**	**9**
Ti1-O1	1.823(2)	1.841(2)	1.854(3)
Ti2-O1	1.813(2)	1.802(3)	1.831(4)
Ti1···Ti2	3.050(1)	3.093(1)	3.266(2)
Ti-N	---	2.089(3)	2.120(5) 2.140(5)
Ti2-C16	2.158(3)	2.147(4)	2.232(6)
N-C	---	1.273(5)	1.273(7) 1.286(8)
Ti-C51/C61	---	2.103(4)	2.090(5) 2.036(6)
Ti-CH_2	2.127(3) 2.117(3) 2.134(3)	2.108(4) 2.212(4)	2.202(5)
Ti1-O1-Ti2	114.1(1)	116.2(1)	124.8(2)
Ti2-C16-C11	104.0(2)	102.7(2)	108.4(3)

The ^{1}H NMR spectra of derivatives **7** and **8** in benzene-d_6 revealed an analogous "tuck-over" splitting pattern to that of complexes **3-6**: one resonance for the η^5-C_5Me_5 ligand, four singlets for the methyl groups and a diastereotopic methylene unit for the (μ-η^5-$C_5Me_4CH_2$-κC) ligand. Analogously, these spectra show two inequivalent methylene groups and two signals for the methyl groups of the Ti-CH_2-CMe_2-CH_2-Ti fragment, according with the asymmetry of **7** and **8**. Further signals were assigned to the

neopentyl, 2,6-dimethylphenyl, and *tert*-butyl substituents of the η^2-iminoacyl moiety. The existence of the η^2-iminoacyl ligands is confirmed by the resonances for the carbon atoms at 247.2 (**7**) and 245.3 (**8**) ppm in the $^{13}C\{^1H\}$ NMR spectrum and a stretching band for the C=N bond at 1566 and 1596 cm^{-1} in the IR spectrum, respectively.[29-35]

On the other hand, we proceeded to carry out the reaction of compound **2** with two equivalents or a slightly excess of *tert*-butyl- or 2,6-dimethylphenyl isocyanides. The reactions were monitored by ^1H NMR spectroscopy in benzene-d_6 at room temperature, showing firstly the formation of **7** and **8**, and later the incorporation of a second isocyanide molecule. While the reaction with the aryl isocyanide generated a complex reaction mixture, an analogous procedure with *tert*-butyl isocyanide evidenced the presence of a new species **9** (see Scheme 2). All attempts to obtain this compound on a preparative scale failed, but a few crystals collected at the bottom of an NMR tube allowed us to elucidate its structure.

The molecular structure of complex **9** is displayed in Figure 3 and selected structural data in Table 2, and shows that the Ti1(μ-η^5-$C_5Me_4CH_2$-κC)Ti2 bonding system is chemically inert when insertion processes are carried out on complex **2** and its derivatives. Now, both metal centers present a four-legged piano stool environment, with the same number of electrons, leading to more similar Ti-O distances, although longer than those found for **2** and **7**, with less steric hindrance. Also, the Ti1-O1-Ti2 bond angle is clearly affected, being ≈10° or 8° wider than those observed for **2** and **7**, respectively, lengthen ≈0.2 Å the Ti1···Ti2 distance. In the same sense, Ti2-C16 elongates 0.08 Å to alleviate the steric congestion, and the Ti-η^2-iminoacil bonding system presents slightly longer distances with respect to **7** although are still in the range found for η^2-iminoacyl titanium complexes.[29-35]

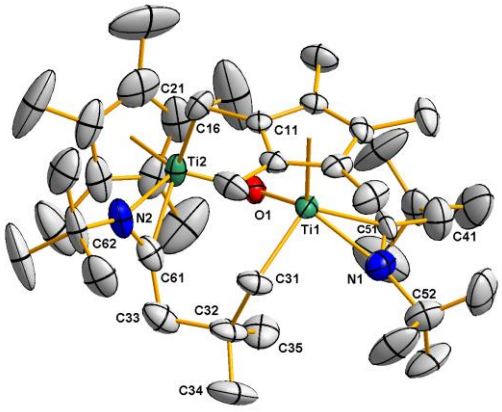

Figure 3. ORTEP plot of **9**. Thermal ellipsoids set at 50% probability. All hydrogen atoms are omitted for clarity.

As previously stated, isocyanide insertions occur exclusively into the titanium-carbon bonds of the terminal benzyl or neopentyl groups of **1** and **2**, and not on the tuck-over ligand. To gain a better understanding of this selective reactivity at a mechanistic level, DFT calculations were performed on the complexes **1** and **2**, and the simplest isocyanide substrate MeNC, as a model.

Figure 4 shows a schematic Gibbs energy diagram with alternate mechanistic scenarios for the insertion of the isocyanide into different Ti-C bonds of compound **1**.

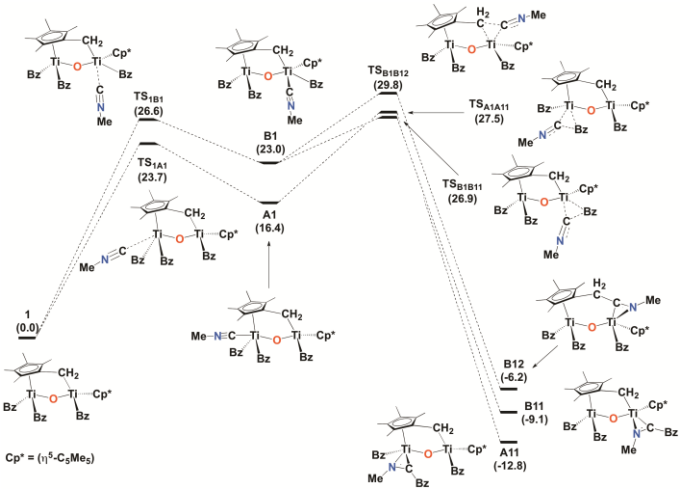

Figure 4: Gibbs energy profile at 25°C (kcal·mol^{-1}) for the insertion of MeNC on complex **1**.

Reactions occur, as previously reported,[29] with a first coordination of the nucleophilic isocyanide to one of the two electron-deficient metal centers and subsequent RNC insertion into the corresponding titanium-carbon bonds with possible formation of different η^2-iminoacyl complexes. In all cases, the stepwise global reactions are computed to be thermodynamically favorable at 25 °C as can be seen in Figure 4. The first step of the process, MeNC binding to both inequivalent Ti atoms is endergonic as a result of the steric hindrance imposed by the addition of the isocyanide ligand to one of the metallic centers in the already sterically congested dimer in conjunction with the bimolecular nature of this associative stage. Calculations show that the approach to the titanium atom linked to two benzyl ligands is kinetically favored by ≈3 kcal mol^{-1} with respect to the approach to the other metal center, leading to a model **A1** intermediate thermodynamically more stable than **B1**. Once these intermediates are formed, they can revert back to the reagents with decoordination of the isocyanide or alternatively, they can overcome transition states **TSA1A11** or **TSB1B11** to yield respectively the **A11** or **B11** insertion products. In spite of a kinetic and thermodynamic preference for **A1** formation, the global kinetic barriers to yield the final **A11** and **B11** η^2-iminoacyl complexes are comparable, $\Delta G^{\ddagger}_{298K}$ = 27.5 and 26.9 kcal mol^{-1} respectively.

It is interesting to observe that the barrier for isocyanide binding and subsequent insertion into the Ti-$CH_2C_5Me_4$ bond generating species $\mathbf{B_{12}}$ through transition state $\mathbf{TS_{B1B12}}$ is also

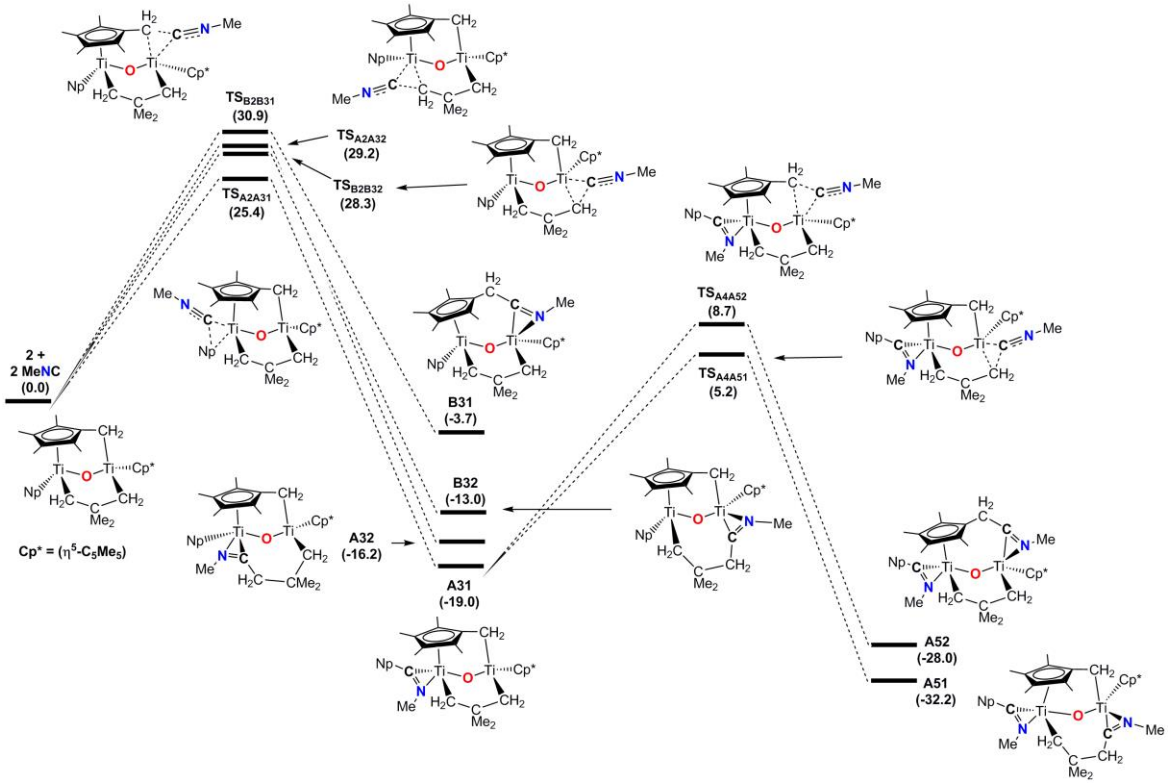

Figure 5: Simplified Gibbs energy profile at 25°C (kcal·mol^{-1}) for the insertion steps of MeNC on complex **2**. A full energy profile can be seen in Figure S11.

moderate ($\Delta G^{\ddagger}_{298K}$ = 29.8 kcal mol^{-1}). However, the other two previously discussed alternatives shown in Figure 4, $\mathbf{A_{11}}$ and $\mathbf{B_{11}}$ formation, are preferred from a kinetic ($\Delta\Delta G^{\ddagger}_{298K}$ = 2-3 kcal mol^{-1}) and thermodynamic ($\Delta\Delta G^{\ddagger}_{298K}$ = 3-6 kcal mol^{-1}) global point of view, in agreement with our experimental results. In this sense, we have observed on the crystal structures of **3**, **4** and **5** that the insertion process let us to isolate only complexes of $\mathbf{A_{11}}$- or $\mathbf{B_{11}}$-type depending on the isocyanide employed.

The reaction mechanism for the insertion of isocyanides into Ti-C bonds in compound **2** was also analyzed computationally with the simplest isocyanide model MeNC. The Gibbs Energy profile obtained is essentially identical to that shown in Figure 4 for the insertion of MeNC on complex **1**. A simplified Gibbs energy diagram with the most representative minima and transition states for MeNC insertion on species **2** is presented in Figure 5. A full energy profile can be seen in the Supporting Information (Figure S11). The isocyanide approach again shows two possibilities depending on the Ti center where the incoming ligand attacks. Binding to the metal bearing a terminal Np ligand is less endergonic (ΔG^{0}_{298K} = 16.2 kcal mol^{-1}) and more kinetically favorable ($\Delta G^{\ddagger}_{298K}$ = 18.6 kcal mol^{-1}) than binding of the isocyanide to the Ti center with a Cp* ligand (ΔG^{0}_{298K} = 21.6 kcal mol^{-1} and $\Delta G^{\ddagger}_{298K}$ = 23.2 kcal mol^{-1}), similarly as it has already been discussed above for compound **1**.

The insertion of MeNC into the terminal Ti-Np bond of **2** with formation of complex **A31** is the preferred pathway and exhibit a kinetic barrier for the whole process, isocyanide binding and insertion, of $\Delta G^{\ddagger}_{298K}$ = 25.4 kcal·mol^{-1}, 1.5-2.0 kcal·mol^{-1} lower than that computed for complex **1** (see Figure 4). At 25 ºC, the alternative insertions into the Ti-$CH_2C_5Me_4$ or Ti-(μ-$CH_2CMe_2CH_2$) bonds are less exergonic and present higher computed barriers, as shown in Figure 5. Again, the isocyanide insertion on the "tuck-over" ligand is computed to be the less thermodynamically and kinetically favored transformation. As it can be checked, the structure of the preferred species, **A31**, as predicted by DFT-calculations, is in agreement with that experimentally obtained for complex **7** (see Figure 2).

Next, we studied the possible path for a second insertion process. Once the first molecule of isocyanide had been incorporated on one of the titanium atoms yielding complex **A31** as shown in Figure 5, the approach of the second MeNC was oriented to the other metal center, less electronically saturated and sterically hindered. As shown in Figure 5, the following step, insertion of the isocyanide, can be performed into the Ti-$CH_2C_5Me_4$ or Ti-(μ-$CH_2CMe_2CH_2$) bonds. Both possibilities present moderate to low energy barriers, but the latter insertion is kinetically preferred by 3.5 kcal mol^{-1} leading to the thermodynamically most stable complex **A51**. Not surprisingly, the structure of **A51** matches with that crystallographically determined for complex **9** (see Figure 3).

CONCLUSION

The species **1** and **2** show a remarkable inertness in isocyanides insertion processes on the titanium-carbon bond of the tuck-over functionality. In contrast, the reactivity of these species with isocyanides takes place on the Ti-alkyl bonds. DFT calculations support this selective reactivity observed experimentally and show a kinetic and thermodynamic preference for isocyanide insertion reactions into the titanium-alkyl bonds of complexes **1** and **2** over the alternative insertion into the "tuck-over" ligand.

EXPERIMENTAL SECTION

General Procedures. All operations were performed in a M. Braun double drybox or using vacuum standard Schlenk techniques under argon atmospheres. Toluene and hexane were freshly distilled under argon from sodium and sodium/potassium alloy, respectively. Benzene-d_6 was dried with Na/K alloy, vacuum distilled and stored under argon. [$Ti_2(\eta^5$-$C_5Me_5)(CH_2Ph)_3(\mu$-η^5-$C_5Me_4CH_2$-$\kappa C)(\mu$-O)] (**1**) and [$Ti_2(\eta^5$-$C_5Me_5)(CH_2CMe_3)(\mu$-η^5-$C_5Me_4CH_2$-$\kappa C)(\mu$-$CH_2CMe_2CH_2)(\mu$-O)] (**2**) were prepared according to the literature.[28] The isocyanides RNC, R = 2,6-$Me_2C_6H_3$, Me_3SiCH_2, *t*Bu, *i*Pr, were purchased by Aldrich and used as received. Infrared spectra were prepared as samples in KBr pellets on the FT-IR Perkin-Elmer SPECTRUM 2000 and IR-FT Perkin-Elmer Frontier spectrophotometers. CHN analyses were performed with a Perkin-Elmer 2400-Series II C, H, N, S/O. ^{1}H and ^{13}C NMR spectra were obtained by using Varian NMR System spectrometers: Unity-300 Plus, Mercury-VX and Unity-500, and reported with reference to solvent resonances (residual C_6D_5H in benzene-d_6, 7.15 ppm (^{1}H) and 128.0 ppm (^{13}C)). ^{1}H-^{13}C gHSQC were recorded from benzene-d_6 solutions using a Unity-500 MHz NMR spectrometer operating at 25 °C.

General procedure for the synthesis of the compounds **3**-**8**. A 25 mL-Schlenk was charged with **1** (200 mg, 0.31 mmol) or **2** (200 mg, 0.38 mmol) and were solved in 15-20 mL of hexane or toluene. RNC (R = Xyl, Me_3CH_2, *t*Bu, *i*Pr) was added slowly in small portions. The reaction mixture was stirred for a few minutes, filtered, concentrated up to approx. 5 ml and immediately was cooled at -20 °C for several days. After filtration, the microcrystalline solid was dried in vacuum and stored at -20 °C.

Synthesis of complexes 3 and 4. **1** (200 mg, 0.31 mmol) and XylNC (40 mg, 0.31 mmol) or Me_3CH_2SiNC (45 μL, 36 mg, 0.31 mmol) were solved in toluene (**3**) or hexane (**4**) and were placed in a 25 mL-Schlenk to yield dark red crystals of **3** (139 mg, 57%) or orange reddish crystals of **4** (124 mg, 52%).

3: IR (KBr, cm^{-1}): $\bar{\nu}$ = 3061 (w), 3020 (w), 2955 (m), 2906 (vs), 2861 (m), 1592 (m, C=N), 1564 (m,), 1487 (m), 1448 (m), 1378 (m), 1207 (m), 1173 (m), 1093 (m), 1027 (m), 745 (m), 710 (vs), 655 (w), 618 (w), 594 (w), 528 (w). Satisfactory NMR spectra could not be obtained due to rapid decomposition in solution. Elemental analysis (%) calcd. for $C_{50}H_{59}NOTi_2$ (785.74): C, 76.43; H, 7.57; N, 1.78; found: C, 76.32; H, 7.59; N, 1.74.

4: IR (KBr, cm^{-1}): $\bar{\nu}$ = 3061 (w), 2905(s), 1585 (s, C=N), 1486 (m), 1444 (w), 1375 (m), 1253 (m), 1201 (m), 1096 (w), 1023 (m), 966 (m), 849 (s), 800 (w), 745 (vs), 703 (vs), 589 (w), 510 (m). 427 (w). ^{1}H NMR (C_6D_6, 300 MHz, 298 K): δ = 7.56-6.86 (m, 15H, Ph), 3.68 (s, 2H, CH_2), 3.16, 3.02 (AB syst., 2H, ^2J = 13.0 Hz, CH_2), 2.60 (s, 2H, CH_2), 2.22, overlapping (2H, ^2J = 11.7 Hz, CH_2), 2.10, 1.82, 1.56, 1.05, (s, 3H, $C_5Me_4CH_2$), 1.82 (s, 15H, η^5-C_5Me_5), 1.36, overlapping (2H, ^2J = 11.7 Hz, CH_2), -0.01 (s, 9H, CH_2SiMe_3). Elemental analysis (%) calcd. for $C_{46}H_{61}NOSiTi_2$ (767.80): C, 71.96; H, 8.01; N, 1.82; found: C, 71.92; H, 7.90; N, 1.95.

Synthesis of complexes 5 and 6. A solution of **1** (200 mg, 0.31 mmol) and *t*BuNC (35 μL, 26 mg, 0.31 mmol) or *i*PrNC (30 μL, 22 mg, 0.31 mmol) in hexane were placed in a 25 mL-Schlenk to yield orange crystals of **5** (92 mg, 40%) or orange reddish crystals of **6** (79 mg, 35%).

5: IR (KBr, cm^{-1}): $\bar{\nu}$ = 3053 (w), 2905 (s), 1639 (m), 1592 (s, C=N), 1484 (s), 1447 (m), 1363 (m), 1263 (m), 1207 (m), 1029 (m), 977 (w), 802 (s), 746 (vs), 711 (vs), 696 (vs), 655 (w), 506 (w), 468 (w), 388 (s). ^{1}H NMR (C_6D_6, 500 MHz, 298 K): δ = 7.75-6.75 (m, 15H, Ph), 3.97, 3.79 (AB syst., 2H, ^2J = 18.0 Hz, CH_2), 2.63, 1.81 (AX syst., 2H, ^2J = 10.0 Hz, CH_2), 2.53, 1.93 (AX syst., 2H, ^2J = 10.5 Hz, CH_2), 2.09, 1.72, 1.74, 1.56 (s, 3H, $C_5Me_4CH_2$), 2.36, 1.85 (AX syst., 2H, ^2J = 10.0 Hz, CH_2), 1.69 (s, 15H, η^5-C_5Me_5), 1.28 (s, 9H, CMe_3). Elemental analysis (%) calcd. for $C_{46}H_{59}NOTi_2$ (737.70): C, 74.89; H, 8.06; N, 1.90; found: C, 74.89; H, 8.19; N, 3.20.

6: IR (KBr, cm^{-1}): $\bar{\nu}$ = 3055 (w), 3015 (w), 2955(w), 2911 (w), 2848 (w), 1593 (s, C=N), 1485 (m), 1447 (w), 1376 (m), 1214 (m), 1204 (m), 1027 (m), 967 (w), 798 (m), 744 (vs), 692 (vs), 625 (w), 445 (m). ^{1}H NMR (C_6D_6, 500 MHz, 298 K): δ = 7.55-6.85 (m, 15H, Ph), 3.95 (ht, 1H, ^3J = 6.5 Hz, CHMe$_2$), 3.68, 3.39 (AB syst., 2H, ^2J = 15.0 Hz, CH_2), 2.56, 2.46 (AB syst., 2H, ^2J = 10.0 Hz, CH_2), 2.10, 1.90, 1.51, 1.05 (s, 3H, $C_5Me_4CH_2$), 1.87 (s, 15H, η^5-C_5Me_5), 2.11, 2.05 (AB syst., 2H, ^2J = 10.0 Hz, CH_2), 1.84, 1.28 (AX syst., 2H, ^2J = 15.0 Hz, CH_2), 1.13 (d, 3H, ^3J = 6.5 Hz, CHMe*Me*), 0.84 (d, 3H, ^3J = 6.5 Hz, CH*Me*Me). Elemental analysis (%) calcd. for $C_{45}H_{57}NOTi_2$ (723.67): C, 74.69; H, 7.94; N, 1.94; found: C, 75.02; H, 7.79; N, 1.11.

Synthesis of complexes 7 and 8. **2** (200 mg, 0.38 mmol) and XylNC (50 mg, 0.38 mmol) or *t*BuNC (45 μL, 33 mg, 0.39 mmol) were solved in hexane and were placed in a 25 mL-Schlenk to yield dark red microcrystalline solid of **7** (235 mg, 95%) or reddish microcrystalline solid of **8** (193 mg, 84%).

7: IR (KBr, cm^{-1}): $\bar{\nu}$ = 2944 (s), 2894 (s), 2864 (s), 1566 (m, C=N), 1437 (m), 1376 (m), 1363 (m), 1203 (m), 1172 (m), 1093 (w), 1022 (d), 766 (m), 699 (vs), 652 (w), 624 (w), 599 (w), 585 (w), 510 (w), 427 (w). ^{1}H NMR (C_6D_6, 500 MHz, 298 K): δ = 7.05 (t, 1H, ^3J = 4.5 Hz, 2,6-Me_2Ph), 6.97 (d, 2H, ^3J = 4.5 Hz, 2,6-Me_2Ph), 2.50, 2.30 (AB syst., 2H, ^2J = 14.5 Hz, CH_2), 2.37, 1.90 (s, 3H, 2,6-*Me*$_2$Ph), 2.32, 1.98, 1.82, 1.52 (s, 3H, $C_5Me_4CH_2$), 2.08, 1.12 (AX syst., 2H, ^2J = 15.5 Hz, CH_2), 1.92 (s, 15H, η^5-C_5Me_5), 1.65, 1.53 (AB syst., 2H, ^2J = 12.0 Hz, CH_2), 2.03, 0.01 (AX syst., 2H, ^2J = 12.0 Hz, CH_2), 1.24, 1.13 (s, 3H, CMe_2), 1.04 (s, 9H, CH_2CMe_3). ^{13}C{^{1}H} NMR (C_6D_6, 125 MHz, 298 K): δ = 247.2 (XylN*C*), 146.4-125.0 (2,6-Me_2*Ph*NC), 126.2-116.0 (*C*$_5$Me$_4$CH$_2$), 120.4 (η^5-*C*$_5$Me$_5$), 98.9, 63.8, 56.4, 50.2 (*C*H$_2$), 20.3, 19.4 (2,6-*Me*$_2$PhNC), 14.6, 14.2, 13.1, 11.5 ($C_5Me_4CH_2$), 45.2, 36.7 ($CH_2CMe_2CH_2$), 30.9 (C*Me*$_3$), 54.9, not observed (*C*Me$_3$ and $CH_2CMe_2CH_2$), 11.8 (η^5-C_5Me_5). Elemental analysis (%) calcd. for $C_{39}H_{59}NOTi_2$ (653.62): C, 71.66; H, 9.10; N, 2.14; found: C, 71.40; H, 8.96; N, 2.17.

8: IR (KBr, cm^{-1}): $\bar{\nu}$ = 2937(s), 2902 (s), 1596 (s, C=N), 1374 (m), 1362 (s), 1231 (w), 1157 (w), 1194 (m), 1021 (w), 803 (w), 707 (vs), 655 (w), 618 (w), 566 (w), 544 (s), 425 (w). ^{1}H NMR (C_6D_6, 500 MHz, 298 K): δ = 3.15, 2.25 (AX syst., 2H, ^2J = 14.5 Hz, CH_2), 2.29, 1.83, 1.70, 1.47 (s, 3H, $C_5Me_4CH_2$), 2.15, 1.02 (AX syst., 2H, ^2J = 11.0 Hz, CH_2), 1.97 (s, 15H, η^5-C_5Me_5), 1.53, 1.35 (AX syst., 2H, ^2J = 11.5 Hz, CH_2), 2.13, -0.13 (AX syst., 2H, ^2J = 12.5 Hz, CH_2), 1.43 (s, 9H, CMe_3), 1.09 (s, 9H, CH_2CMe_3). ^{13}C{^{1}H} NMR (C_6D_6, 125 MHz, 298 K): δ = 245.0 (*t*BuN*C*), 127.1, 123.4, 118.2, 117.1, not observed (*C*$_5$Me$_4$CH$_2$), 120.2 (η^5-*C*$_5$Me$_5$), 98.0, 65.9, 54.0, 49.5 (*C*H$_2$), 62.6 (*C*Me$_3$), 54.5 (CH_2CMe_3), 32.5 ($CH_2CMe_2CH_2$), 45.5, 35.0 (C*Me*$_2$), 31.0, 30.6 (C*Me*$_3$), 14.2, 13.6, 12.7, 11.8 ($C_5Me_4CH_2$), 11.8 (η^5-C_5Me_5). Elemental analysis (%) calcd. for $C_{35}H_{59}NOTi_2$ (605.58): C, 69.42; H, 9.82; N, 2.31; found: C, 69.34; H, 10.91; N, 2.39.

Crystallography. Crystals of **3**, **4**, **5**, **7** and **9** were obtained as described along the text. Crystals were removed from the Schlenks and covered with a layer of a viscous perfluoropolyether (FomblinY). A suitable crystal was selected with the aid of a microscope, mounted on a cryoloop, and immediately placed in the low-temperature nitrogen stream of the diffractometer. The intensity data sets were collected at 200 K on a Bruker-Nonius KappaCCD diffractometer equipped with an Oxford Cryostream 700 unit. Crystallographic data for all complexes are

presented in Table S1. The structures were solved, by using the WINGX package,[43] by direct methods (SHELXS-2013)[44,45] and refined by least-squares against F^2 (SHELXL-2017).[44,45] Each molecule of compound **4** crystallized with half disordered molecule of hexane and no sensible chemical model could be obtained, thus Squeeze[46] procedure was used to remove its contribution to the structure factors. All non-hydrogen atoms were anisotropically refined, while hydrogen atoms were placed at idealized positions and refined using a riding model. Molecules of **7** presented disorder in the C21-C30 pentamethylcyclopentadienyl ligand; two sites were found for each carbon atom with optimized occupancies of 54% and 46% respectively, EADP[44,45] restraints were also applied to obtain a sensible chemical model.

Computational Details. Electronic structure calculations were performed using the B3LYP density functional[47-49] and the LANL2DZ basis set and associated pseudopotential for Ti[50,51] and a standard 6-31G(d) basis set for the rest of the atoms. We refer to this basis set combination in this work as BSI. Geometry optimizations were performed without any symmetry restrictions, and all stationary points were optimized by computing analytical energy gradients. The obtained minima were characterized by performing energy second derivatives, confirming them as minima by the absence of negative eigenvalues of the Hessian matrix of the energy. Transition states were characterized by single imaginary frequency, whose normal mode corresponded to the expected motion. To further refine the energies obtained from the B3LYP/BSI calculations, single-point calculations were performed using the larger LANL2TZ basis set with an additional *f* polarization function[52] and 6-311+G(2d,p) basis set for Ti and the rest of the atoms respectively. We refer to this basis set combination in this work as BSII. To determine ΔG°(298 K) values, computed electronic energies obtained using the larger BSII basis set were corrected for zero-point energy, thermal energy and entropic effects estimated from the normal mode analysis using the smaller BSI basis set. The reliability of the thermodynamic and kinetic data computed by this approach has been previously assessed for a series of related molecules and processes.[28] All calculations were performed with the Gaussian 09 suite of programs.[53]

ASSOCIATED CONTENT

Supporting Information

The Supporting Information is available free of charge on the ACS Publications website.

Table of crystallographic data for **3**, **4**, **5**, **7** and **9** (Table S1).

π-stacking interactions in compound **3** (Figure S1).

Structural parameters related to the π-stacking interaction in **3** (Table S2).

NMR spectra for complexes **4**-**8** (Figures S2-S10).

Cartesian coordinates for theoretical calculations (XYZ) and full energy profile for the insertion steps of MeNC on complex **2** (Figures S11).

Accession Codes

CCDC 1831377-1831381 contain the supplementary crystallographic data for this paper. These data can be obtained free of charge via www.ccdc.cam.ac.uk/data_request/cif, or by emailing data_request@ccdc.cam.ac.uk, or by contacting The Cambridge Crystallographic Data Centre, 12 Union Road, Cambridge CB2 1EZ, UK; fax: +44 1223 336033.

AUTHOR INFORMATION

Corresponding Author

* Email: cristina.santamaria@uah.es

Notes

The authors declare no competing financial interest.

ACKNOWLEDGMENT

Financial support for this work was provided by the Ministerio de Economía y Competitividad (CTQ2013-44625-R and CTQ2016-80600-P) and the Universidad de Alcalá (CCG2016/EXP-009). M. G.-P. and J. I. G.-P. thank the Universidad de Alcalá for a doctoral fellowship.

REFERENCES

(1) McDade, J. C.; Green, J. C.; Bercaw, J. E. A Kinetic and Mechanistic Study of the Thermolysis of Bis(pentameth ylcyclopentadienyl)dimethyltitanium(IV). *Organometallics* **1982**, *1*, 1629-1634.

(2) Bercaw, J. E.; Marvich, R. H.; Bell, L. G.; Brintzinger, H. H. Titanocene as an Intermediate in Reactions Involving Molecular Hydrogen and Nitrogen. *J. Am. Chem. Soc*. **1972**, *94*, 1219-1238.

(3) Bercaw, J. E. Bis(pentamethylcyclopentadienyl)titanium(II) and Its Complexes with Molecular Nitrogen. *J. Am. Chem. Soc*. **1974**, *96*, 5087-5095.

(4) Watson, P. L.; Parshall, G. Organolanthanides in Catalysis. *Acc. Chem. Res*. **1985**, *18*, 51-56.

(5) Watson, P. L. Methane Exchange Reactions of Lanthanide and Early-Transition-Metal Methyl Complexes. *J. Am. Chem. Soc*. **1983**, *105*, 6491-6493.

(6) For a comprehensive review on pentafulvene complexes, see: Preethalayam, P.; Krishnan, K. S.; Thulasi, S.; Chand, S. S.; Joseph, J.; Nair, V.; Jaroschik, F.; Radhakrishnan, K. V. Recent Advances in the Chemistry of Pentafulvenes. *Chem Rev*. **2017**, *117*, 3930–3989.

(7) Schock, L. E.; Brock, C. P.; Marks, T. J. Intramolecular Thermolytic C-H Activation Processes. Solid-State Structural Characterization of a Mononuclear η^6-$Me_3C_5CH_2$ Zirconium Complex and a Mechanistic Study of Its Formation from $(Me_5C_5)_2Zr(C_6HH_5)_2$. *Organometallics* **1987**, *6*, 232-241.

(8) Thompson, M. E.; Baxter, S. M.; Bulls, A. R.; Burger, B. J.; Nolan, M. C.; Santarsiero, B. D.; Schaefer, W. P.; Bercaw, J. E. "σ Bond Metathesis" for C-H Bonds of Hydrocarbons and Sc-R (R = H, alkyl, aryl) Bonds of Permethylscandocene Derivatives. Evidence for Noninvolvement of the π System in Electrophilic Activation of Aromatic and Vinylic C-H Bonds. *J. Am. Chem. Soc.* **1987**, *109*, 203-219.

(9) Bulls, A. R.; Schaefer, W. P.; Serfas, M.; Bercaw, J. E. Intramolecular C-H Bond Activation of Benzyl Ligands by Metalated Cyclopentadienyl Derivatives of Permethylhafnocene. Molecular Structure of $(\eta^5$-$C_5Me_5)(\eta^5,\eta^1$-$C_5Me_4CH_2)HfCH_2C_6H_5$ and the Mechanism of Rearrangement to Its Hafnabenzocyclobutane Tautomer $(\eta^5$-$C_5Me_5)_2HfCH_2$-o-C_6H_4. *Organometallics* **1987**, *6*, 1219-1226.

(10) den Haan, K. H.; Teube, J. H. Formation of a Novel Yttrium Hydride with Bridging 1,2,3,4-Tetramethylfulvene and Hydride Ligands. *J. Chem. Soc., Chem. Commun.*, **1986**, 682-683.

(11) Pattiasina, J. W.; Hissink, C. E.; de Boer, J. L.; Meetsma, A.; Teuben J. H. Formation of a Novel η^3:η^4-1,2,3-Trimethyl-4,5-dimethylenecyclopentenyl Ligand by Hydrogen Abstraction from a Permethylcyclopentadienyl Group in Permethyl titanocene Carbyl and Related Systems. *J. Am. Chem. Soc.* **1985**, *107*, 1158-1159.

(12) Cloke, F. G. N.; Green, J. C.; Green, M. L. H.; Morley, C. P. Metal Atom Synthesis and Photochemistry of Bis(η-

pentamethylcyclopentadienyl)tungsten Dihydride. *J. Chem. Soc., Chem. Commun*., **1985**, 945-946.

(13) Werner, H.; Crisp, G. T.; Jolly, P. W.; Kraus, H. J.; Kruger, C. Synthesis of (1,2,3,4-Tetramethylfulvene)palladium(0) Complexes from (η^5-Pentamethylcyclopentadienyl)palladium(II) Precursors. The Crystal Structure of $[Pd(PMe_3)_2(\eta^2\text{-}CH_2{=}C_5Me_4)]$. *Organometallics* **1983**, *2*, 1369-1377.

(14) Bottomley, F.; Lin, I. J. B.; White, P. S. Di-μ-oxo-(η^1:η^5-1,2,3,4-tetramethyl-5-methylene-1,3-cyclopentadienebis[(η-pentamethylcyclopentadienyl)titanium], $(\mu\text{-}O)2[\mu\text{-}[\eta^1{:}\eta^5\text{-}C_5(CH_2)(CH_3)_4][Ti[\eta^5\text{-}C_5(CH_3)_5]]_2$, a Complex Containing a Bridging Tetramethylmethylenecyclopentadienyl Ligand. *J. Am. Chem. Soc*., **1981**, *103*, 703-704.

(15) Pinkas, J.; Císarová, I.; Horácek, M; Kubista, J.; Mach, K. Reactions of Hydrogen Sulfide with Singly and Doubly Tucked-in Titanocenes. *Organometallics*, **2011**, *30*, 1034-1045.

(16) Janssen, T.; Severin, R.; Diekmann, M.; Friedemann, M.; Haase, D.; Saak, W.; Doye, S.; Beckhaus R. Bis(η^5:η^1-pentafulvene)titanium Complexes: Catalysts for Intramolecular Alkene Hydroamination and Reagents for Selective Reactions with N -H Acidic Substrates. *Organometallics* **2010**, *29*, 1806-1817.

(17) Pinkas, J.; Císarová, I.; Gyepes, R.; Horácek, M; Kubista, J.; Cejka, J.; Gómez-Ruiz, S.; Hey-Hawking, E.; Mach, K. Insertion of Internal Alkynes and Ethene into Permethylated Singly Tucked-in Titanocene. *Organometallics*, **2008**, *27*, 5532-5547.

(18) Beweries, T.; Burlakov, V. V.; Peitz, S.; Bach, M. A.; Arndt, P.; Baumann, W.; Spannenberg, A.; Rosenthal U. Reactions of Decamethylhafnocene with 1,3-Butadiynes: Formation of Hafnacyclocumulenes and C-H Activation at Pentamethyl cyclopentadienyl Ligands. *Organometallics*, **2007**, *26*, 6827-6831.

(19) Sun, Y.; Spence, R. E. v. H.; Piers, W. E.; Parvez, M.; Yap G. P. A. Intramolecular Ion -Ion Interactions in Zwitterionic Metallocene Olefin Polymerization Catalysts Derived from "Tucked-In" Catalyst Precursors and the Highly Electrophilic Boranes $XB(C_6F_5)_2$ (X = H, C_6F_5). *J. Am. Chem. Soc.* **1997**, *119*, 5132-5143.

(20) Fandos, R.; Teuben, J. H.; Helgesson, G.; Jagner, S. Reactivity of Early-Transition-Metal Fulvene Complexes. Transformation of a 2,3,4,5-Tetramethylfulvene Ligand into a Bidentate Dialkoxide with Four Asymmetric Carbon Atoms. Molecular Structure of $Ti[(OCHPh)_2C_5Me_4(CH_2)]Cl_2$. *Organometallics*, **1991**, *10*, 1637-1639.

(21) Pattiasina, J. W.; Bolhuis, F. v.; Teuben J. H. Titanium Hydride Formation through Hydrogen Transfer from 2-Methylpyridine to a Titanium Fulvene Compound;the First Structurally Characterized Terminal Titanium Hydride. *Angew, Chem. Int Ed. Engl*. **1987**, *26*, 330-331.

(22) Hamilton, D. M. Jr.; Willis, W. S.; Stucky, G. D. Synthesis, Structural Characterization, and Molecular Orbital Calculations for a Titanium Lewis Acid Carbonyl Adduct. *J. Am. Chem. Soc.* **1981**, *103*, 4255-4256.

(23) Bercaw, J. E.; Brintzinger, H. H. Bis(pentamethylcyclopentadienyl)titanium(II). Isolation and Reactions with Hydrogen, Nitrogen, and Carbon Monoxide. *J. Am. Chem. Soc.* **1971**, *93*, 2045-2046.

(24) Bottomley, F.; Egharevba, G. O.; Lin, I. J. B.; White, P. S. Preparation, Structure, and Reactivity of a (Pentamethylcyclopentadienyl)titanium Dimer Bridged by Oxygen and Tetramethylmethylenecyclopentadienyl. *Organometallics*, **1985**, *4*, 550-553.

(25) Evans, W. J.; Champagne, T. M.; Ziller, J. W. Organolutetium Vinyl and Tuck-Over Complexes via C-H Bond Activation. *J. Am. Chem. Soc.* **2006**, *128*, 14270-14271.

(26) Arnold, P. L.; McMullon, M. W.; Rieb, J.; Khn F. E. C-H Bond Activation by f-Block Complexes. *Angew. Chem. Int. Ed.* **2015**, *54*, 82-100.

(27) Johnson, K. R. D.; Hayes, P. G. Cyclometalative C–H bond activation in rare earth and actinide metal complexes. *Chem. Soc. Rev*. **2013**, *42*, 1947–1960.

(28) Carbó, J. J.; García-López, D.; Gómez-Pantoja, M.; González-Pérez, Juan I.; Martín, A.; Mena, M.; Santamaría, C. Intermetallic Cooperation in C–H Activation Involving Transient Titanium-Alkylidene Species: A Synthetic and Mechanistic Study. Organometallics **2017**, 36, 3076–3083.

(29) Boyarskiy, V. P.; Bokach, N. A.; Luzyanin, K. V.; Kukushkin, V. Y. Metal-Mediated and Metal-Catalyzed Reactions of Isocyanides. *Chem. Rev.* **2015**, *115*, 2698-2779.

(30) Fandos, R.; Otero, A.; Rodríguez, A. M.; Suizo, S. Monocyclopentadienyl titanium complexes supported by functionalized Shiff Base ligands. *J. Organomet. Chem.* **2014**, *759*, 74-82.

(31) Trunkely, E. F.; Epshteyn, A.; Zavalij, P. Y.; Sita, L. R. Synthesis, Structural Characterization, and Preliminary Reactivity Profile of a Series of Monocyclopentadienyl, Monoacetamidinate Titanium(III) Alkyl Complexes Bearing β-Hydrogens. *Organometallics* **2010**, *29*, 6587–6593.

(32) Xu, T.; Gao, W.; Mu, Y.; Ye, L. Synthesis and characterization of a novel η^2-iminoacyl monocyclopentadienyl titanium(IV) complex. *J. Coord. Chem.* **2007**, *60*, 2533–2539.

(33) Fandos, R.; Gallego, B.; Otero, A.; Rodríguez, A.; Ruiz, M. J.; Terreros, P.; Pastor, C. A new titanium building block for early–late heterometallic complexes; preparation of a new tetrameric metallomacrocycle by self assembly. *Dalton Trans.*, **2006**, 2683–2690.

(34) Scott, M. J.; Lippard, S. J. Isocyanide Insertion Reactions with Organometallic Group 4 Tropocoronand Complexes: Formation of η^2-Iminoacyl, Enediamido, η^2-Imine, and μ-Imido Products. *Organometallics* **1997**, *16*, 5857–5868.

(35) Durfee, L. D.; Rothwell, I. P. Chemistry of η^2-Acyl, η^2-Iminoacyl, and Related Functional Groups. *Chem. Rev*. **1988**, *88*, 1059-1079.

(36) Roesky, H. W.; Haiduc, I.; Hosmane, N. S. Organometallic Oxides of Main Group and Transition Elements Downsizing Inorganic Solids to Small Molecular Fragments. *Chem. Rev.* **2003**, *103*, 2579–2595.

(37) Varkey, S. P.; Schormann, M.; Pape, T.; Roesky, H. W.; Noltemeyer, M.; Herbst-Irmer, R.; Schmidt, H.-G. Organotitanoxanes $[C_5Me_5TiMe_2]_2(\mu\text{-}O)$ and $[(C_5Me_5)_4Ti_4Me_2](\mu\text{-}O)_5$: Synthesis and Crystal Structures. *Inorg. Chem*. **2001**, *40*, 2427–2429.

(38) Gómez-Sal, P.; Martín, A.; Mena, M.; Yélamos, C. Synthesis of the Organotitanoxane Complexes $[(\eta^5\text{-}C_5Me_5)_4Ti_4X_2](\mu\text{-}O)_5$. X-ray Structure of $[(\eta^5\text{-}C_5Me_5)_4Ti_4Me_2](\mu\text{-}O)_5$. *Inorg. Chem*. **1996**, *35*, 242–243.

(39) Andrés, R.; Galakhov, M.; Gómez-Sal, M. P.; Martín, A.; Mena, M.; Santamaría, C. Allyl derivatives of $[\{Ti(\eta^5\text{-}C_5Me_5)(\mu\text{-}O)Cl)\}_3]$: X-ray crystal structure of $[(Ti\{\eta^5\text{-}C_5Me_5)(\mu\text{-}O)(CH_2CH{=}CHMe)\}_3]$. *J. Organomet. Chem.* **1996**, *526*, 135–143.

(40) Gómez-Sal, P.; Mena, M.; Palacios, F.; Royo, P.; Serrano, R.; Martínez-Carreras, S. Preparation of the compounds $(\mu\text{-}O)[Ti(C_5Me_5)R_2]_2$ (R = Me, CH_2Ph, or CH_2SiMe_3) and the crystal structure of the derivative with R = CH_2SiMe_3. *J. Organomet. Chem*. **1989**, *375*, 59–65.

(41) Serrano, R.; Flores, J. C.; Royo, P.; Mena, M.; Pellinghelli, M. A.; Tiripicchio, A. Polynuclear η^2-Benzophenone Methylhydrazonato(1-) Complexes from the Insertion of Ph_2CN_2 into Ti-CH_3 Bonds of Electron-Deficient Organotitanium Oxides. X-ray Structure of $[Ti(C_5Me_5)Me(\eta^2\text{-}MeNNCPh_2)][Ti(C_5Me_5)Me_2](\mu\text{-}O)$. *Organometallics* **1989**, *8*, 1404–1408.

(42) García-Blanco, S.; Gómez-Sal, M. P.; Martínez-Carreras, S.; Mena, M.; Royo, P.; Serrano, R. Hydrolytic Studies on $(\eta^5\text{-}C_5Me_5)TiMe_3$; X-Ray Structure of $[(\eta^5\text{-}C_5Me_5)TiMe(\mu\text{-}O)]_3$ containing a Ti_3O_3 Ring. *J. Chem. Soc., Chem. Commun.* **1986**, 1572–1573.

(43) Farrugia, L. J. WinGX and ORTEP for Windows: an update. *J. Appl. Crystallogr.* **2012**, *45*, 849–854.

(44) Sheldrick, G. M. Crystal structure refinement with

SHELXL. *Acta Crystallogr*. **2015**, *C71*, 3–8.

(45) Sheldrick, G. M. A short history of SHELX. *Acta Crystallogr., Sect. A: Found. Crystallogr.* **2008**, *64*, 112–122.

(46) Spek, A. L. PLATON SQUEEZE: a tool for the calculation of the disordered solvent contribution to the calculated structure factors. *Acta. Cryst*. **2015**, *C71*, 9-18.

(47) Stephens, P. J.; Devlin, F. J.; Chabalowski, C. F.; Frisch, M. J. Ab Initio Calculation of Vibrational Absorption and Circular Dichroism Spectra Using Density Functional Force Fields. *J. Phys. Chem*. **1994**, *98*, 11623-11627.

(48) Becke, A. D. Densityfunctional thermochemistry. III. The role of exact exchange. *J. Chem. Phys.* **1993**, *98*, 5648-5652.

(49) Lee, C. T.; Yang, W. T.; Parr, R. G. Development of the Colle-Salvetti correlation-energy formula into a functional of the electron density. *Phys. Rev. B* **1988**, *37*, 785-789.

(50) Hay P. J.; Wadt, W. R. Ab initio effective core potentials for molecular calculations. Potentials for the transition metal atoms Sc to Hg. *J. Chem. Phys*. **1985**, *82*, 270-283.

(51) Hay P. J.; Wadt, W. R. Ab initio effective core potentials for molecular calculations. Potentials for K to Au including the outermost core orbitals. *J. Chem. Phys*. **1985**, *82*, 299-310.

(52) Roy, L. E.; Hay, P. J.; Martin, R. L. Revised Basis Sets for the LANL Effective Core Potentials. *J. Chem. Theory Comput*. **2008**, *4*, 1029-1031.

(53) Gaussian 09, Revision D.01, Frisch, M. J.; Trucks, G. W.; Schlegel, H. B.; Scuseria, G. E.; Robb, M. A.; Cheeseman, J. R.; Scalmani, G.; Barone, V.; Mennucci, B.; Petersson, G. A.; Nakatsuji, H.; Caricato, M.; Li, X.; Hratchian, H. P.; Izmaylov, A. F.; Bloino, J.; Zheng, G.; Sonnenberg, J. L.; Hada, M.; Ehara, M.; Toyota, K.; Fukuda, R.; Hasegawa, J.; Ishida, M.; Nakajima, T.; Honda, Y.; Kitao, O.; Nakai, H.; Vreven, T.; Montgomery, Jr., J. A.; Peralta, J. E.; Ogliaro, F.; Bearpark, M.; Heyd, J. J.; Brothers, E.; Kudin, K. N.; Staroverov, V. N.; Kobayashi, R.; Normand, J.; Raghavachari, K.; Rendell, A.; Burant, J. C.; Iyengar, S. S.; Tomasi, J.; Cossi, M.; Rega, N.; Millam, J. M.; Klene, M.; Knox, J. E.; Cross, J. B.; Bakken, V.; Adamo, C.; Jaramillo, J.; Gomperts, R.; Stratmann, R. E.; Yazyev, O.; Austin, A. J.; Cammi, R.; Pomelli, C.; Ochterski, J. W.; Martin, R. L.; Morokuma, K.; Zakrzewski, V. G.; Voth, G. A.; Salvador, P.; Dannenberg, J. J.; Dapprich, S.; Daniels, A. D.; Farkas, Ö.; Foresman, J. B.; Ortiz, J. V.; Cioslowski, J.; Fox, D. J. Gaussian, Inc. Wallingford CT, 2013.

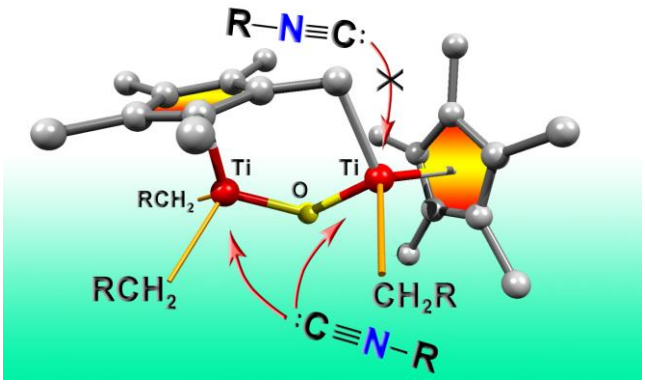
R–N≡C:
Ti
Ti
O
RCH2
RCH2
CH2R
:C≡N–R